Acta Chemica Scandinavica A 39 (1985) 593– 604

A Time Resolved Powder Neutron Diffraction Investigation of Reactions of Portland Cement Components with Water

A. NØRLUND CHRISTENSEN,[a] H. FJELLVÅG[b] and M.S. LEHMANN[b]

[a] Department of Inorganic Chemistry, Aarhus University, DK-8000 Aarhus C, Denmark and [b] Institut Max von Laue – Paul Langevin, F-38042 Grenoble Cedex, France

The reactions between D_2O and the Portland cement clinker components Ca_3SiO_5, β-Ca_2SiO_4, and Ca_2AlFeO_5 were investigated by on-line powder neutron diffraction methods at temperatures up to 120 °C. The only crystalline reaction product found in the reaction of Ca_3SiO_5 with water is $Ca(OD)_2$. The reaction of β-Ca_2SiO_4 is much slower than that of Ca_3SiO_5. The crystalline reaction products of the reaction of Ca_2AlFeO_5 with water are $Ca(OD)_2$ and $Ca_3Al_2(OD)_{12}$. The activation energy for the formation of $Ca_3Al_2(OD)_{12}$ in the Ca_2AlFeO_5-D_2O reaction is 58.2 kJ/mol.

The reaction rates of hydration for compounds of the type $Ca_xAl_yO_z$ are related to the relative content of calcium ions. Compounds with high calcium content react faster with water than compounds with low calcium content. Some correlations between reactivity and crystal structures are discussed.

Heterogeneous mixtures of solids and water described as cement pastes or cement mortars comprise a wide range of chemical systems, each with typical ways of reaction. This work is restricted to hydration reactions of solid compounds relevant to Portland cement clinker. This material, however, shows wide variations with respect to composition due to differences between available raw materials. The main components (oxides) of two representative types of cement clinker are given in Table 1. Tricalcium silicate Ca_3SiO_5, dicalcium silicate β-Ca_2SiO_4, tricalcium aluminate $Ca_3Al_2O_6$, and Brownmillerite Ca_2AlFeO_5, are the main components. In contact with water these crystalline phases generally undergo hydration reactions yielding new crystalline hydrated phases and amorphous gels.[2,3] These processes in the cement mortars provoke solidification during a few hours, whereas the final strength properties are only attained after a number of weeks.

Table 1. Representative compositions (%) of Portland cement clinker (Aalborg Portland).[1]

Oxides	Low-alkali cement	Rapid cement
Ca_3SiO_5	60	58
Ca_2SiO_4	26	20
$Ca_3Al_2O_6$	1.5	8.6
Ca_2AlFeO_5	9.2	9.0
CaO (free)	0.6	1.1

0302-4377/85 $2.50

Table 2. Short-hand notations for mixed oxides and hydroxides discussed in the text.

$C_3S \equiv Ca_3SiO_5$	$C_3A \equiv Ca_3Al_2O_6$	$CA \equiv CaAl_2O_4$
$\beta\text{-}C_2S \equiv \beta\text{-}Ca_2SiO_4$	$C_{12}A_7 \equiv Ca_{12}Al_{14}O_{33}$	$CA_2 \equiv CaAl_4O_7$
$C_4AF \equiv Ca_2AlFeO_5$	$C_5A_3 \equiv Ca_5Al_6O_{14}$	$C_3AD_6 \equiv Ca_3Al_2(OD)_{12}$

The results of a study of reactions between water and the pure calcium oxides $Ca_3Al_2O_6$, $Ca_{12}Al_{14}O_{33}$, $CaAl_2O_4$, and $CaAl_4O_7$ were published in Ref. 4. Due to the large number of simultaneous reactions it is difficult to ascribe measured quantities to a particular chemical reaction for Portland cement. Hence, in this investigation the more convenient approach of studying reactions between water and some pure oxides was first adopted. As a second step, different additives were included into these reactions. The outcome of the latter studies will be published separately. A large number of investigations on hydration of Portland cement mortars and on selected cement clinker compounds have been reported using a variety of methods (*e.g.* measurements of heat evolution,[5] X-ray diffraction,[6] small-angle scattering,[7] SEM,[8,9] TEM[8,9,10] and registration of mechanical properties[11]). In many cases the reaction products have only been studied at certain time intervals after having been brought to ambient conditions.

This work deals with the hydration properties of Ca_3SiO_5, $\beta\text{-}Ca_2SiO_4$, and Ca_2AlFeO_5. In the present investigation, using on-line powder neutron diffraction measurements of characteristic scattered intensities from reactants and products, the chemical changes are recorded in real time and the chemical reactions proceed in the sample holder simultaneously with the diffraction measurements.

The abbreviations commonly used in cement chemistry literature by referring to the compositions in terms of double oxides, are adopted. Setting *C* for CaO, *A* for Al_2O_3, *F* for Fe_2O_3, *S* for SiO_2, and *D* for D_2O (*H* for H_2O) the short hand notation for the relevant phases are as listed in Table 2.

EXPERIMENTAL

(i) *Sample preparation and characterization.* C_4AF was made by zone melting of stoichiometric mixtures of the oxides in a crystal growth furnace. Chemicals used were Al_2O_3, Fe_2O_3 (Merck, analytical grade) and CaO made from $CaCO_3$ (Merck, analytical grade). The calcium carbonate was kept for 8 h at 1000 °C in a crucible furnace to produce CaO.

It turned out to be impossible to synthesize C_3S and $\beta\text{-}C_2S$ from stoichiometric amounts of the pure oxides CaO and SiO_2 (amorphous, Elkem). This is in accordance with the fact that C_3S is metastable below 1250 °C, while pure $\beta\text{-}C_2S$ is metastable relative to $\gamma\text{-}C_2S$ below 675 °C but can be stabilized by minor quantities of oxide additives. The calcium silicates in cement clinker contain minor amounts of other oxides that act as stabilizers for C_3S and $\beta\text{-}C_2S$. The present C_3S sample was made from a mixture of 0.71 mol CaO, 0.23 mol amor phous SiO_2, 0.006 mol γ-FeOOH (Minnesota Mining and Manufacturing Company), 0.005 mol Al_2O_3, 0.025 mol MgO (Lycal, technical grade), and 0.011 mol MnF_2 (Riedel, technical grade), corresponding to a product which is quoted as "Alite"; it will, however, be denoted as C_3S here. The finely ground mixtures of these compounds were heated in a MgO crucible at 1440 °C for 20 h. The advantage of using amorphous SiO_2 is increased reactivity, the additions of MgO, Fe_2O_3, and Al_2O_3 stabilize the C_3S phase while the presence of manganese fluoride reduces the formation temperature to approximately 1100 °C.[13]

$\beta\text{-}C_2S$ was made similarly from a mixture of 0.40 mol CaO, 0.17 mol crystalline SiO_2 (Merck, analytical grade), 0.7 mmol Al_2O_3, and 0.4 mmol Fe_2O_3. After crushing and

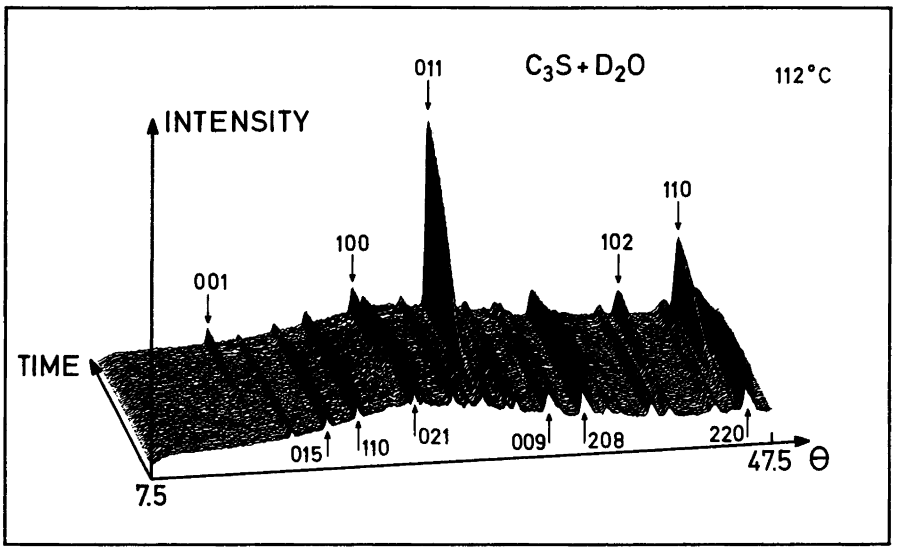

Fig. 1. Powder neutron diffraction diagrams of C_3S–D_2O mixture at 112 °C recorded with 20 min intervals. Miller indices for selected reflections of C_3S ↑ (refer to pseudocell) and $Ca(OD)_2$ ↓ are indicated.

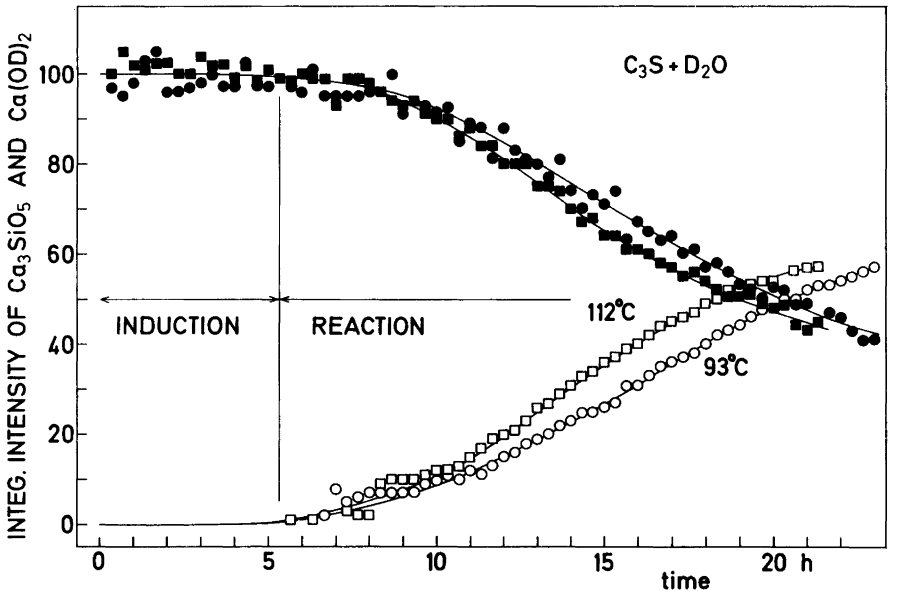

Fig. 2. Integrated intensities of C_3S (●, ■) and $Ca(OD)_2$ (○, □) *vs.* time for the reaction of C_3S with D_2O at 93 and 112 °C. The intensities of C_3S and $Ca(OD)_2$ are on relative scales. Estimated uncertainty 4 %.

mixing, the products were pressed isostatically to 5 cm long rods that were heated in MgO crucibles in a furnace at 1315 °C for 48 h. Upon cooling, the rods broke down as powders due to the conversion of α-C_2S into γ-C_2S. This powder was reheated in order to increase the β-C_2S/γ-C_2S ratio,[14] first at 400 °C for 8 h, next at 1000 °C for 8 h. This heat treatment was repeated once and the sample was finally kept at 400 °C for 8 h before cooling to room temperature over 1 h. At that stage the sample contained only minor impurities of γ-C_2S and CaO.

The fractions of the samples which passed a 150 mesh sieve were used for the hydration experiments studied by on-line neutron diffraction. No further information on the particle size is at hand. The quality of the starting materials was checked by Guinier photographs using Cu$K\alpha_1$ radiation and Si as internal standard. All starting materials gave sharp Guinier photographs. X-Ray powder diffraction data were also recorded for the end products of the hydration experiments.

(ii) *Powder neutron diffraction.* Powder neutron diffraction data were collected on the D1B diffractometer at the Laue-Langevin Institute, using neutrons of wavelength 2.517 Å (evaluated using $C_{12}A_7$ as standard; a=11.989(1) Å). The diffractometer has a 400-cell multidetector covering 80 ° in 2θ. In a typical experiment, 3.00 g solid was mixed with 3.75 ml D_2O (99.7 %) in an 11 mm-diameter vanadium container. The container, sealed with an indium gasket, was placed in a thermostated vanadium oven with a temperature stability of ±1 °C. The large sample and beam size ensure representative measurements of the bulk reactions, which otherwise might be a problem in experiments using X-ray radiation. The recorded intensities were extracted at 5, 10 or 20 min intervals, depending on the actual reaction rate. The evolution in real time of a chemical reaction is visualized[15] in Fig. 1, which shows how the intensities of Bragg reflections from the crystalline starting material C_3S and the reaction product $Ca(OD)_2$ change in time. Miller indices are given for selected Bragg peaks. The main features of such reactions can equally well be presented as the time dependence of integrated intensities[16] of selected reflections. This is exemplified in Fig. 2.

RESULTS

(i) *Hydration of calcium silicates.* The hydration of C_3S can generally be divided into three steps,[17,18] respectively denoted initialization, induction and reaction ranges, *cf.* Fig. 2.

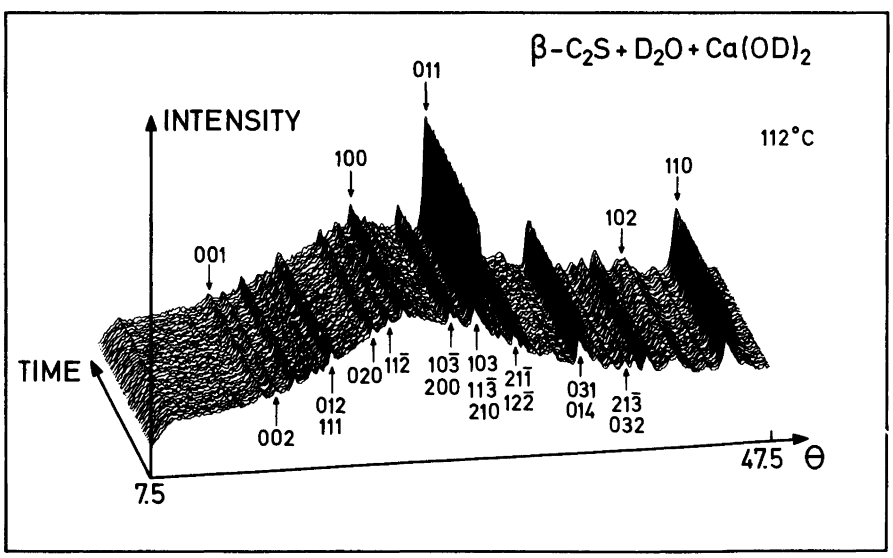

Fig. 3. Powder neutron diffraction diagrams of a β-C_2S–$Ca(OD)_2$–D_2O mixture at 112 °C recorded with 20 min intervals. Miller indices for β-C_2S ↑ and $Ca(OD)_2$ ↓ are included.

According to Refs. 17, 18 a rapid dissolution of a small amount of C_3S takes place in the initialization step immediately after the solid is brought in contact with water. However, the C_3S amount consumed in this step is so small (1–2 %) that it could not be resolved in the present experiment. At least two explanations for the following induction (dormant) period prevail;[19] either a reduced nucleation rate of hydration products [amorphous *C-S-D* gel and $Ca(OD)_2$] is the cause, or else the presence of a protective layer surrounding the grains for a certain time explains the facts. The onset of the reaction period, after 5–6 h, is characterized by precipitation of $Ca(OD)_2$.

$Ca(OD)_2$ is the only crystalline reaction product, *cf.* Figs. 1 and 2. In Fig. 2 the intensities of $Ca(OD)_2$ have been normalized to 50 for the measured value 50 of the C_3S intensity, assuming equal reaction rates for the precipitation of $Ca(OD)_2$ and the dissolution of C_3S. The total reaction can be written as[20]

$$2Ca_3SiO_5 + 7D_2O \rightleftarrows Ca_{2x}(OD)_{4x-2}D_4Si_2O_7+(6-2x)\ Ca(OD)_2;\ 2>x>1$$

All 'silicon oxide' from the dissolution of C_3S is found in the amorphous *C-S-D* gels. The hydration rate attains its maximum value during the reaction periods investigated. The maximum is shifted towards longer times by reducing the temperature, *viz.* at ~ 12 and ~ 17 h for 112 and 93 °C, respectively. When discussing the hydration properties of C_3S attention should be paid to the fact that the amount of impurities introduced during the syntheses will affect the reactivity.

For β-C_2S the hydration rate is less than for C_3S in conformity with earlier findings.[21,22] Fig. 3 shows the real time evolution of the diffraction pattern of a mixture of β-C_2S/$Ca(OD)_2$/D_2O at 112 °C and only minor changes are observed. Similar data collected at 102 and 120 °C confirm these findings.

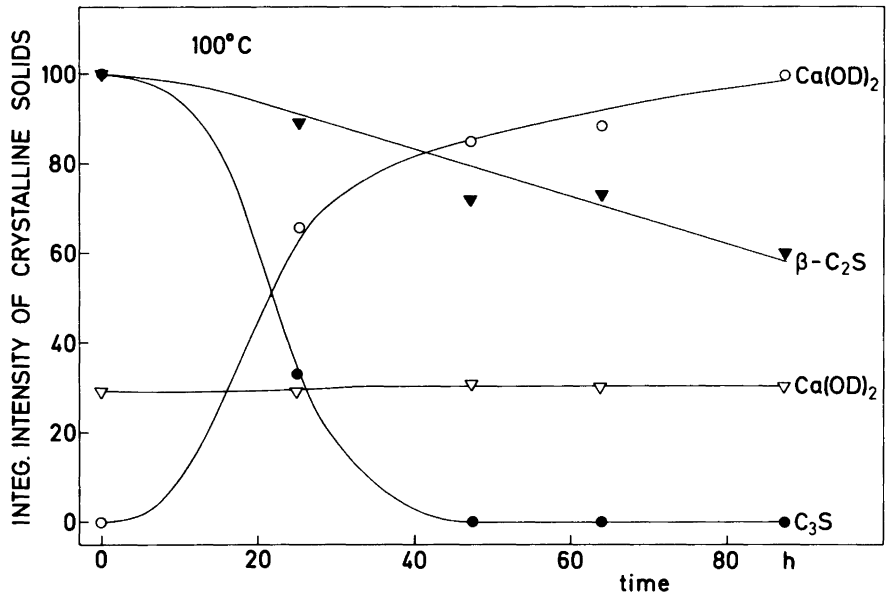

Fig. 4. Integrated intensity of C_3S (●), β-C_2S (▼) and $Ca(OD)_2$ (○,▽) *vs.* time for reactions between C_3S and D_2O or β-C_2S and D_2O at 100 °C.

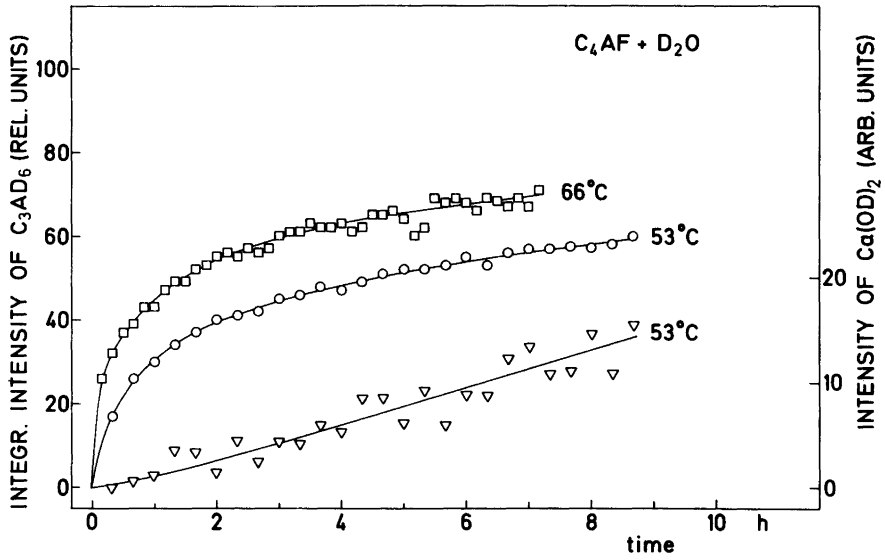

Fig. 5. Integrated intensity of C_3AD_6 (○, □) *vs.* time for reactions between C_4AF and D_2O at 53 and 66 °C. A representative curve for the crystallization of $Ca(OD)_2$ (at 53 °C) is included (▽).

In order to obtain data for longer hydration times than allowed by an on-line experiment, relevant sample mixtures containing C_3S, β-C_2S (with a small $Ca(OD)_2$ excess) and D_2O were heated at 100 °C for longer periods of time. The heat treatments were only interrupted for the time necessary to record powder neutron diffraction intensities. The results in Fig. 4 show that β-C_2S reacts more slowly with D_2O than does C_3S.

(ii) *Hydration of Brownmillerite.* Brownmillerite, C_4AF belongs to a solid solution series comprising CaO, Al_2O_3, and Fe_2O_3 [$Ca_4(Al_xFe_{1-x})_4O_{10} \equiv C_4A_{2x}F_{2-2x}$; $x \leq 0.69$]. The hydration properties of the phase are reported to vary slightly with composition (x). The reaction rates are higher for A rich samples. Other C-F phases like CF, CF_2 were not studied since they are not relevant for the properties of Portland cement. The refined unit cell parameters for the C_4AF sample used is a=5.546(1), b=14.460(3), c=5.325(1) Å; space group *Ibm*2, indexing based on calculated intensities using the program LAZY-PULVERIX.[23] The unit cell dimensions obtained correspond to samples more rich in A than C_4AF according to Refs. 24, 25.

Results from the hydration experiments of C_4AF are displayed in Figs. 5 and 6. At temperatures between 53 and 103 °C, one of the crystalline reaction products is a cubic phase (C_3AD_6) of the hydrogarnet type.[26,27] When C_4AF is brought in contact with water, the integrated intensities of C_4AF reflections are, during a short time, reduced significantly, and C_4AF resembles in this manner C_3A. A small amount of C_4AF remained unreacted throughout the experiments, probably because large grains become protected by rapid overgrowth of reaction products. The curve in Fig. 6 for C_4AF at 103 °C is representative for all the C_4AF experiments. C_3AD_6 (hydrogrossular) is the main reaction product from hydrolysis of calcium aluminates, however it forms easily solid solution series, among these $Ca_3Al_{2-x}Fe_x(OD)_{12}$. Least-squares refinements based on Guinier photographs of a C_4AF sample completely hydrolysed at 80 °C for 48 h give a cell constant a=12.592(1) compared to

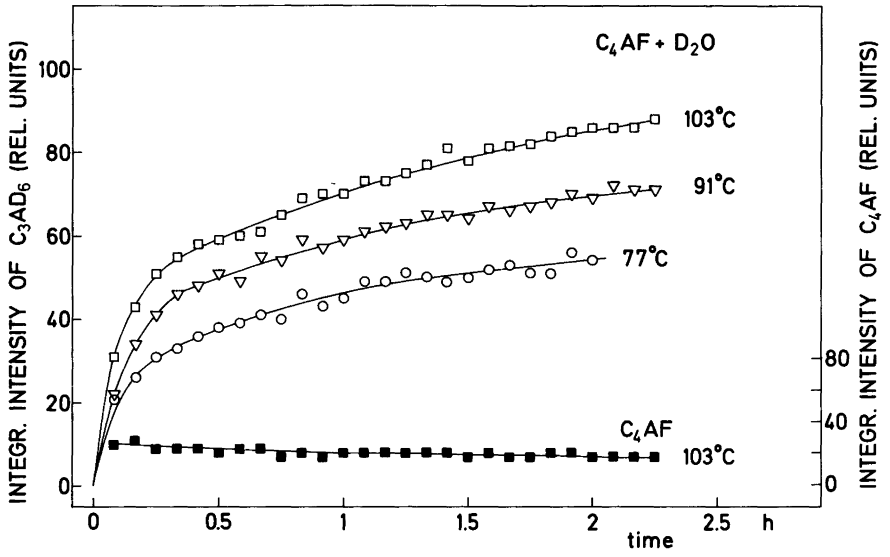

Fig. 6. Integrated intensity of C_4AF (■) and C_3AD_6 (○,▽,□) *vs.* time for reactions between C_4AF and D_2O at 77, 91, and 103 °C.

12.571(2) Å for pure C_3AD_6. This is in agreement with corresponding values derived from the neutron diffraction data (a=12.635(3) and 12.574(2) Å) and indicates that the obtained reaction product contains only slight amounts of iron. The unit cell parameter for $Ca_3Al_{2-x}Fe_x(OD)_{12}$ is reported to vary approximately linearly with x, being 12.76 Å for C_3FD_6.[28] A comparison of observed and calculated Bragg intensities of the solid solution phase further confirmed the reaction products to be C_3AD_6 and $Ca(OD)_2$. The precipitation of $Ca(OD)_2$ also suggests that nearly all Fe will be in the amorphous part of the sample, as calcium would otherwise be used in the formation of C_3FD_6 or of $Ca_3Al_{2-x}Fe_x(OD)_{12}$ with a high content of Fe: $C_4AF+7D_2O \rightarrow C_3AD_6 + Ca(OD)_2 +$ "Fe_2O_3" (amorphous). In this respect,Brownmillerite differs from C_3A since the latter does not precipitate $Ca(OD)_2$ upon hydrolysis.[4]

DISCUSSION

The powder neutron diffraction studies show that the hydration properties of *C-A**, *C-S*, and *C-A-F* phases differ considerably. A measure of the reactivity in the hydration of a compound is the time ($t_{0.5}$) required for consumption (production) of half of the amount of reactants (products). Table 3 presents the results of $t_{0.5}$ deduced from the neutron diffraction studies. In a number of cases are $t_{0.5}$ (product) > $t_{0.5}$ (reactant), that is the reactants are nearly completely consumed before any crystalline products are observed. This is the case for C_3A, C_4AF, and to a less pronounced extend for CA. It is observed that the values of $t_{0.5}$ (reactant) decreases with increasing C/A ratio in the *C-A* series of compounds. The reduced reactivity of *C-S* phases relative to *C-A* phases are evident from the corresponding $t_{0.5}$ values. The hydration reactions of C_3S, CA_2, and possibly as well of CA are characterized by

* The compound $C_{12}A_7$ was erroneously quoted as C_5A_3 in Ref. 4.

Table 3. Time (*h*) necessary for reducing (increasing) the quantity of reactants (products) to half their maximum value.

Starting material	T(°C)	$t_{0.5}$(reactant)	$t_{0.5}$(product)
C_3S	93	20.3	~20
β-C_2S	100	~100	>>100
C_4AF	53	0.5	4.6
	66	0.4	1.5
C_3A	49	<0.1	0.3
	63	<0.1	0.12
$C_{12}A_7$	49	1.9	2.0
	63	0.3	0.3
CA	49	3.5	>7.0
	63	1.3	3.5
CA_2	49	50.0[a]	>50.0[a]
	93	3.5	3.5

[a] Extrapolated.

an induction period. The reason for this has been discussed above. The large span in $t_{0.5}$ values for the various main constituents of Portland cement clinker (*cf.* Tables 1 and 3) are reflected in time dependent mechanical properties of the end products.

A more detailed understanding of the nature of the reactions is gained from a study of the time dependence of $\alpha(t)$, where $\alpha(t)$ is the degree of hydration at time t. The reactions are heterogeneous between water and powdered materials. In this case, the changing geometry of the reaction interfaces and diffusion paths will dominate the reaction rate expressions. When the reaction interface moves at a constant rate, the kinetics are said to be linear and the rate varies as the area of the reaction interface. Parabolic kinetics involve a rate control by mass transport through a layer on the particle. The term diffusion controlled kinetics is also used for this case. A general kinetic equation is

$$\alpha(t)=\frac{(k\cdot t)^n}{r}$$

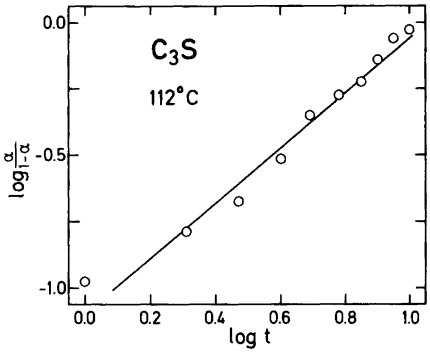

Fig. 7. Display of log $\alpha/(1\text{-}\alpha)$ *vs.* log t for the reaction of C_3S with D_2O at 112 °C.

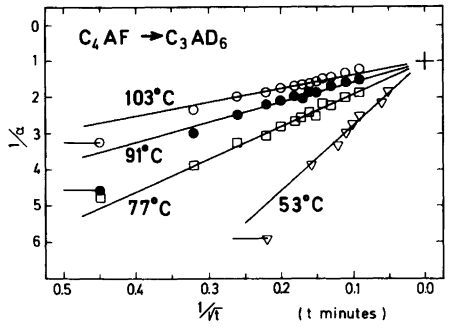

Fig. 8. The inverse degree of hydration $(1/\alpha)$ *vs.* the inverse square root of time $(1/\sqrt{t})$ for reactions of C_4AF with D_2O.

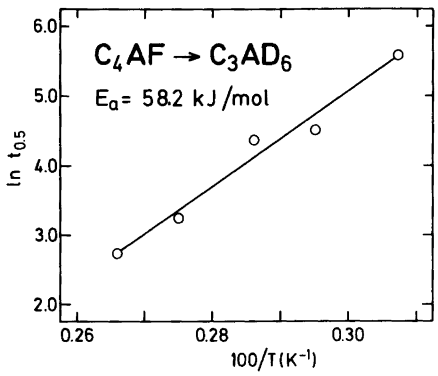

Fig. 9. Arrhenius plot of ln $t_{0.5}$ *vs* 100/*T* for the formation of C_3AD_6 from the reactions of C_4AF with D_2O. Estimated uncertainty in E_a 10 %.

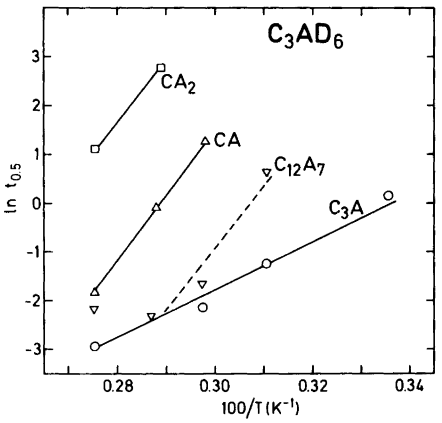

Fig. 10. Arrhenius plot of ln $t_{0.5}$ *vs.* 100/*T* for production of the hydration product C_3AD_6 in the reactions of C_3A, $C_{12}A_7$, CA, and CA_2 with D_2O.

where k is a rate constant, t is time, and r is a measure of the particle size.[29] The linear kinetic corresponds to $n=1$, and the parabolic to $n=\frac{1}{2}$. A quantitative distinction between linear and parabolic kinetics can be obtained from plots of log $\alpha(t)$ *vs.* log t, but for a qualitative distinction inspections of the $\alpha(t)$ *vs.* t plots are sometimes sufficient. Figs. 2 and 6 represent linear and parabolic reaction kinetics of the hydration processes, respectively. When the polydispersity of the particles are included in the kinetic equation[29]

$$\alpha=\alpha(t)=\frac{t^n}{t^n+1/BK^n}$$

where t is measured from the end t_0 of any dormant period, B is a dispersion constant, and K a rate constant. The expression may be rewritten to

$$\log \alpha/(1-\alpha)=n \log (t-t_0)+\text{constant}$$

that can be used to estimate the value of n.

For a more detailed discussion, C_3S will first be considered. The hydration reaction of C_3S is characterized by a long induction period (here $t_0=9$ h). Several model descriptions for the hydration of C_3S have been forwarded, however, it has been pointed out that conclusions based on details of the hydration [$\alpha(t)$] curves are limited by dominating effects of the intrinsic particle size distribution.[29] Thus the data obtained for C_3S are analyzed according to the dispersion model.[29] For C_3S is a plot of log $\alpha/(1-\alpha)$ *vs.* log t shown in Fig. 7 and the linear relationship (*viz.* $n=1$) suggests reaction controlled kinetics.

The hydration curves of C_4AF differ from those of C_3S in the way that they have a negative curvature throughout the reaction period. The time dependance of $\alpha(t)$ for C_4AF determined by the formation of C_3AD_6 is shown in Fig. 8, where $1/\alpha$ is plotted against $1/\sqrt{t}$. The data points fall on straight lines in accordance with a diffusion controlled kinetic description of the formation of C_3AD_6 from C_4AF. Ideally, the lines should pass through the point $1/\alpha=1$, $1/t^{1/2}=0$. They do so when the first data point of each measurement is omitted.

It seems acceptable to do so as these points are determined with the greatest uncertainty in t and α.

The hydration of C_4AF was performed at different temperatures (Figs. 5,6) and the determinations of $t_{0.5}$ were used to estimate the activation energy of the formation of C_3AD_6 from C_4AF as 58.2 kJ/mol from an Arrhenius plot[29] of ln $t_{0.5}$ *vs.* $100/T$, see Fig. 9. Similar Arrhenius plots are shown in Fig. 10 for the hydration of the calcium aluminates, yielding activation energies for the reactions (formation of C_3AD_6) as follows: For C_3A 40 kJ/mol while for $C_{12}A_7$, CA and CA_2 approximately 105 kJ/mol. The variation in the derived values for the activation energies indicates probably that the reaction products, here including the amorphous gels, and hence the mechanisms are different for the phases studied.[4] The compounds with a high C/A ratio (C_3A and C_4AF) apparently have low activation energies, and the compounds with low C/A ratio ($C_{12}A_7$, CA and CA_2) have high activation energies for the formation of C_3AD_6.

The large variations in reactivity of the various phases studied here [*cf.* $t_{0.5}$(reactant) in Table 3] are believed to be reflected by details of the crystal structures. However, the properties of the amorphous intermediate gels may blurr any clear structural correlation with reactivity. By considering the stoichiometry of crystalline reactants and products it is evident that A rich gels prevail in the hydration products of $C_{12}A_7$, CA, and CA_2 while S rich gels are common for C_3S and β-C_2S. Only for C_3A the reactant and product (C_3AD_6) have the same proportion of C and A.

For the C-A compounds values for ln $t_{0.5}$(reactant) and various geometrical parameters are summarized in Fig. 11. A common feature of the crystal structures adopted by the reactant phases, is a framework of connected XO_4 tetrahedra (X=Al, Si, Fe), *cf. e.g.* the constancy of the averaged Al–O distances for calcium aluminates shown in Fig. 11. The coordination of Ca^{2+} with the oxygen atoms is less regular and the Ca–O distances vary considerably both within a given CaO_x polyhedron (from 2.258 to 2.569 Å for C_3A, from 2.360 to 2.523 Å for $C_{12}A_7$, *etc.*) and with the C/A ratio. The way of packing of the AlO_4

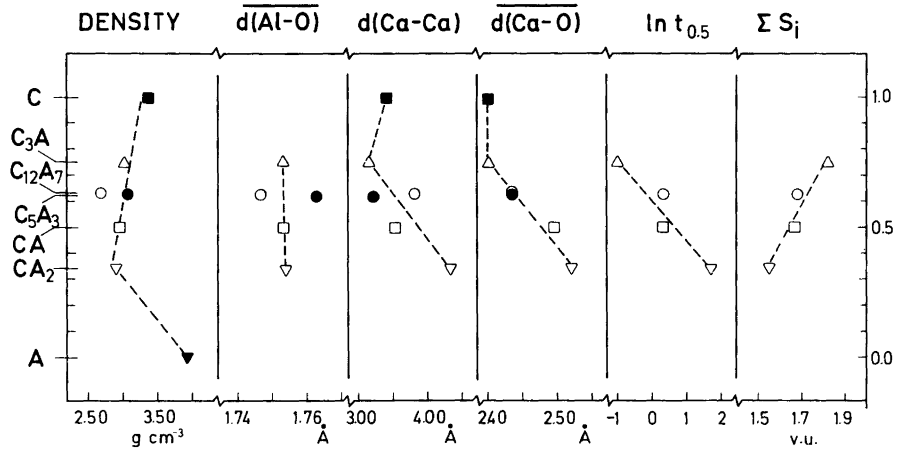

Fig. 11. Interatomic distances (mean CaO_6, mean AlO_4, shortest Ca–Ca) for C_3A,[32] $C_{12}A_7$,[33] C_5A_3,[34] CA,[35] CA_2,[36] A,[37] and C[38] as well as log $t_{0.5}$ and S_i for the CaO–Al_2O_3 compounds. (The Al–O distances in α-Al_2O_3 are 1.86 and 1.97 Å). The symbols indicate C (■), C_3A (△), $C_{12}A_7$ (○), C_5A_3 (●), CA (□), CA_2 (▽), and A (▼). The ordinate indicates mole fraction of compounds from pure A to pure C.

building blocks (tetrahedra) as well as the way of incorporation of Ca^{2+} into larger holes (channels) in the framework differ considerably between the *C-A* compounds. A high *C/A* ratio corresponds to a relative large fraction of the structure being occupied by Ca^{2+} ions and thus to a denser packing of these ions which in turn is reflected in the minimum Ca–Ca distance as well in the mean Ca–O bond lengths (see Fig. 11).

The reaction rates of the $Ca_xAl_yO_z$ compounds with water thus appear to have the greatest values for the phases with the highest calcium content and appear to correlate with the shortest Ca–Ca distances and the average Ca–O distances of the phases (Fig. 11). The hypothesis was tested that a correlation to reactivity also existed with the total bond strength of the Ca–O bonds. The individual bond strength S_i introduced by Pauling[30] is related to the bond length using the expression employed by Brown and Shannon[31] as $S_i=S_o(\bar{R}/R_i)^N$, where R_i is the Ca–O distance and the other symbols have the values[31] $S_o=0.25$ v.u. (valence units), $N=6$, and $\bar{R}=2.468$ Å. The electrostatic valence principle[30] states that the sum of the bond strengths is equal to the valence. For Ca^{2+} the valence is expected to be 2 v.u. Fig. 11 shows bond strengths for Ca^{2+} between 1.55 and 1.82. Compounds with valence for calcium near the value 2 are expected to be the most stable, and an indication for this is found in the values of S_i for the two end products of the hydrolysis, C_3AD_6 and $Ca(OD)_2$ with 1.84 and 1.95 v.u., respectively. The hypothesis of correlation between bond strength and reaction rate of hydrolysis can thus be rejected, as the reactivity of C_3A with water is greater than that of CA_2, while the calculated bond strength of the Ca-O bonds are greater in C_3A than in CA_2.

The structural properties of Ca^{2+} do not alone satisfactorily explain the observed trend in reactivity. Hence, properties connected with the AlO_4-tetrahedra probably also play an important role. A protonic attack on the surface has been suggested to be an important mechanism in the hydrolyses,[19] and the effective charge on the AlO_4-tetrahedra may be a relevant parameter. The result of the hydrolysis is a change of the coordination of Al from tetrahedral to octahedral coordination.

Acknowledgements. Support to this investigation was granted by *The Danish Natural Science Research Council* (ANC), and by *The Royal Norwegian Council for Scientific and Industrial Research* (HF). Mr. N.J. Hansen is acknowledged for assistance in the preparation of the specimens used in the investigation.

REFERENCES

1. Hjorth, L. and Almeborg, J. Aalborg Portland, DK-9100 Aalborg, Denmark. *Personal communication* 1984.
2. Lea, F.M. *The Chemistry of Cement and Concrete,* Edward Arnold Ltd., 3rd Ed., London 1970.
3. Taylor, H.F.W. *The Chemistry of Cement,* Academic, London–New York 1962.
4. Christensen, A.N. and Lehmann, M.S. *J. Solid State Chem. 51* (1984) 196.
5. Adbel Razig, B.E.I., Parker, K.M. and Sharp, J.H. *Therm. Anal. Proc. Int. Conf., 7th 1* (1982) 571.
6. Struble, L.J. *Cement, Concrete and Aggregates, CCAGDP 5* (1983) 62.
7. Winslow, D.N. and Diamond, S. *J. Am. Ceram. Soc. 57* (1974) 193.
8. Breval, E. *Cem. Concr. Res. 6* (1976) 129.
9. Breval, E. *Scand. J. Metall. 6* (1977) 21.
10. Lawrence, F.V., Jr., Reid, D.A. and De Carvalho, A.A. *J. Am. Ceram. Soc. 57* (1974) 144.
11. Mehta, P.K., Pirtz, D. and Polivka, M. *Cem. Concr. Res. 9* (1979) 439.

12. *Gmelins Handbuch der Anorganischem Chemie,* 8. Auflage, Calcium teil B–Lieferung 3, Verlag Chemie, Weinheim 1961, pp. 1037/1038.
13. Ludwig, U. and Wolter, A. *7th International Congress of the Chemistry of Cement, Vol. II,* Paris 1980, p. I-99.
14. Trömel, G. and Möller, H. *Fortschr. Mineralog. 28* (1949) 80.
15. Pannetier, J. *Computer Program P3DD1B,* ILL, Grenoble 1984. *Personal communication.*
16. Wolfers, P. Programs for *Treatment of Powder Profiles,* ILL, Grenoble 1975. *Personal communication.*
17. Fujii, K. and Kondo, W. *J. Am. Ceram. Soc. 57* (1974) 492.
18. Odler, I. and Dörr, H. *Cem. Concr. Res. 9* (1979) 239.
19. Taylor, H.F.W. *10th Intern. Symp. React. of Solids,* Dijon 1984, p. 9.
20. Barret, P. and Bertraudie, D. *10th Intern. Symp. React. of Solids,* Dijon 1984, p. 15.
21. Kantro, D.L. *Transp. Res. Circular 176* (1976) 4.
22. Jost, K.H., Ziemer, B. and Seydel, R. *Acta Crystallogr. B 33* (1977) 1696.
23. Yvon, K., Jeitschko, W. and Parthé, E. *J. Appl. Cryst. 10* (1977) 73.
24. Smith, D.K. *Acta Crystallogr. 15* (1962) 1146.
25. Colville, A.A. and Geller, S. *Acta Crystallogr. B 27* (1971) 2311.
26. Cohen-Addad, C., Ducros, P. and Bertaut, E.F. *Acta Crystallogr. 23* (1967) 220.
27. Foreman, D.W., Jr. *J. Chem. Phys. 48* (1968) 3037.
28. Kuzel, H.-J. *N. Jb. Miner. Mh.* (1968) 87.
29. Knudsen, T. In Young, J.F., Ed., *Characterization and Performance Prediction of Cement and Concrete,* New England College, Henniker, N.H., U.S.A. 1982, p. 125.
30. Pauling, L. *J. Am. Chem. Soc. 51* (1929) 1010.
31. Brown, I.D. and Shannon, R.D. *Acta Crystallogr. A 29* (1973) 266.
32. Mondal, P. and Jeffrey, J.W. *Acta Crystallogr. B 31* (1975) 689.
33. Bartl, H. and Schneller, T. *N. Jb. Miner. Mh.* (1970) 547.
34. Vincent, M.G. and Jeffrey, J.W. *Acta Crystallogr. B 34* (1978) 1422.
35. Hörkner, W. and Müller-Buschbaum, Hk. *J. Inorg. Nucl. Chem. 38* (1976) 983.
36. Goodwin, D.W. and Lindop, A.J. *Acta Crystallogr. B 26* (1970) 1230.
37. Newnham, R.E. and de Haan, Y.M. *Z. Kristallogr. 117* (1962) 235.
38. Primak, W., Kaufman, H. and Ward, R. *J. Am. Chem. Soc. 70* (1948) 2043.

Received March 19, 1985.